



Crystal seed-enhanced ammonia nitrogen and phosphate recovery from landfill leachate using struvite precipitation technique

Addagada Lavanya¹ · Sri Krishnaperumal Thanga Ramesh¹

Received: 15 January 2021 / Accepted: 13 June 2021 / Published online: 22 June 2021
© The Author(s), under exclusive licence to Springer-Verlag GmbH Germany, part of Springer Nature 2021

Abstract

Nitrogen and phosphorous are limiting and crucial elements for all living organisms. The recovery of nitrogen and phosphorous as struvite gained attention due to its ecofriendly fertilizer application. In the present study, feasible recovery of NH_4^+ -N available in the landfill leachate with addition of economically viable waste resources like sewage sludge and Mg^{2+} source as struvite is investigated. However, the fertilizer application of struvite depends upon its purity, which in turn is influenced by pH, molar ratio, and presence of other ions. Laboratory scale studies are conducted to find optimum pH and molar ratio. The results of the studies demonstrated the optimum pH being 9.5 along with PO_4^{3-} -P: Mg^{2+} : NH_4^+ -N molar ratio of 1:1.3:1 is the best condition for struvite formation. To further augment the struvite precipitation kaolinite seed is added to the solution and optimized seed dose is 20 g/L. Existence of Ca^{2+} and Na^+ ions in the solution exhibits a negative impact on struvite precipitation. Response surface methodology is employed to understand the interactive influence of parameters on recovery efficiency. The recovered precipitate consists of 82.5% struvite with PO_4^{3-} -P: Mg^{2+} : NH_4^+ -N ratio 1:1.1:0.9. Also, bioavailability of PO_4^{3-} -P in the recovered precipitate is 89.3%; this signifies high performance of precipitate as fertilizer. Economic assessment highlights that the struvite production is profitable and the profit gained is 159.5\$/m³.

Keywords Sewage sludge · Response surface methodology · Visual MINTEQ · Economic assessment · Bioavailability · Fertilizer

Introduction

Rapid industrialization and urbanization lead to ameliorated living standard throughout the world, which results in generation of large quantity of municipal solid waste (MSW) (Huang et al. 2016). Sanitary landfill is considered as the most economic feasible and accepted method for the disposal of MSW due to simplicity in operation (Ahmed and Lan 2012). Furthermore, landfill also helps to diminish the impact of solid waste on environment by allowing it to degrade under the controlled conditions (Renou et al. 2008). The physical,

chemical, and biological processes occurred during the solid waste degradation process and also percolation of rainfall leads to generation of leachate (Kochany and Lipczynska-Kochany 2009). Additionally, factors such as composition of solid waste, moisture content of solid waste, and soil properties influence the leachate characteristics (Rani et al. 2020). The leachate that is generated from landfill is rich in total ammonia nitrogen (Sun et al. 2015). Hence, it is imperative to collect and treat the landfill leachate appropriately; otherwise, it leads to severe environmental issues.

In general, biological techniques are cost effective for the treatment of landfill leachate (Chemlal et al. 2014). However, greater total ammonia concentration in the leachate notably influences the performance of biological methods. Hence, removal of total ammonia concentration is imperative to improve the performance of biological processes (Di Iaconi et al. 2010). Magnesium ammonium phosphate (MAP) precipitation technique is the most effective and efficient way to remove total ammonia nitrogen (Yu et al. 2012). MAP is also represented as struvite a crystalline material consists of equi molar concentration of ammonium, magnesium and

Responsible Editor: Ta Yeong Wu

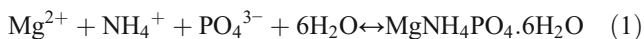
✉ Addagada Lavanya
lavanyaaddagada@gmail.com

Sri Krishnaperumal Thanga Ramesh
stramesh@nitt.edu

¹ Department of Civil Engineering, National Institute of Technology Tiruchirappalli, Tiruchirappalli, Tamil Nadu 620 015, India

phosphate with the formula $\text{MgNH}_4\text{PO}_4 \cdot 6\text{H}_2\text{O}$ (Corona et al. 2020a, b).

Furthermore, struvite is a slow releasing fertilizer and also eco-friendly in nature (Thant Zin and Kim 2019; Min et al. 2019). Moreover, application of struvite as a fertilizer minimizes the N_2O emission from soil when compared with the usage of conventional fertilizers (Chu et al. 2007). The general reaction for struvite precipitation is mentioned below in equation (1).



The major drawback for struvite precipitation is raw material cost (NH_4^+ , Mg^{2+} , PO_4^{3-}) (Yu et al. 2017). Hence, in order to curtail the precipitation cost cheap alternative sources can be used. One among those waste resources is sewage sludge, which is rich in phosphate content (USEPA 2006). Sewage sludge contains 80–90% of phosphate present in sewage (Law and Pagilla 2018). Till present, struvite precipitation has been studied with either nitrogen or phosphate supplied externally as chemical commodities. However, to the best of our knowledge, this is the first study investigating the waste resources as nitrogen and phosphate sources for producing struvite from landfill leachate. In the current study, landfill leachate is used as a nitrogen source whereas sewage sludge is used as a phosphate source for struvite production. Furthermore, to foster the nucleation and growth of struvite crystals, seed material is employed in the present study. In addition to that seed material provides the active sites essential for the nucleation and growth of struvite. Greater surface area to augment nucleation and inertness to the crystallizing solution are the desirable properties of a seed material. Kaolinite is inert to the crystallizing solution; hence, it is used as a seed material in the current study.

Several factors influence the precipitation of struvite includes pH, molar ratio of magnesium, phosphate and ammonia ions and super saturation. In general, the optimum conditions for maximum struvite production would be estimated by varying one parameter while the remaining parameters would be kept as constant. Therefore, it is tedious and time-consuming process. Hence, to overcome the above-mentioned problem researchers started using multivariate statistical models. Among those model's response surface methodology (RSM) is the most commonly used technique for optimization (Lavanya et al. 2019). Moreover, chemical equilibrium model Visual MINTEQ is also utilized to find the speciation and solubility of salts that are likely to exist in the solution. Lavanya and Sri Krishnaperumal Thanga (2020) used RSM and Visual MINTEQ techniques to optimize the phosphate recovery (93.5%) from dairy wastewater includes pH 9.48, MgO:P molar ratio 4:1 and reaction time 73.6 min.

Zhou and Wu (2012) optimized the ammonia removal (1050 mg/L) using RSM and the conditions are Mg:N:P molar ratio 1.26:1:1.11 and pH 9.87.

The current study investigates the feasibility of struvite precipitation using landfill leachate and sewage sludge. The suitability of kaolinite as a seed material to promote the recovery of phosphate and ammonia nitrogen is investigated in the present study. The effect of different parameters such as pH, molar ratio, and seed dose on struvite precipitation is also examined. The overall process optimization is carried out using RSM and Visual MINTEQ is employed to find saturation index of salts. Application potential of recovered precipitate as a fertilizer is also investigated. In addition to that economic viability of the present study is also examined.

Materials and methods

Landfill leachate

The landfill leachate used in the present study is collected from Ariyamangalam, Tamil Nadu, India. Moreover, the age of the landfill leachate is greater than 10 years and is classified as matured or stabilized one. The landfill leachate is collected in 10 L capacity plastic cans and is stored at 4°C to prevent further degradation. The different physico-chemical parameters of landfill leachate are determined using standard methods (APHA 2012). The initial characteristics of collected landfill leachate are given in Table 1.

Sewage sludge characteristics

Sewage sludge used in the present study is collected from municipal sewage treatment plant. The collected sludge is oven dried at 105°C. Then, the sewage sludge is treated with acid (HCl) followed by alkali (NaOH) at liquid to solid ratio of 10. The supernatant obtained after the acid and alkali

Table 1 Initial characteristics of collected landfill leachate

Parameters	Value
pH	7.82
NH_4^+ -N	735.4
PO_4^{3-} -P	18.5
Mg^{2+}	65.8
Ca^{2+}	94.6
Na^+	104
Fe	15.51
Cu	1.23
Ni	0.38
Alkalinity as CaCO_3	5735

* All the values are in mg/L except pH

treatment is characterized using inductivity coupled plasma mass spectrophotometry (ICP-MS). Major elements found in the supernatant were Al (103.1 mg/L), P (472.4 mg/L), K (29 mg/L), Ca (18.1 mg/L), Mg (25 mg/L), Fe (8 mg/L) and trace quantities of Ni (0.01 mg/L), Cu (0.12 mg/L), and Zn (0.9 mg/L).

Seed composition

The composition of kaolinite (i.e., seed material) used in the current study includes O (53.60%), Al (21.40%), Si (22.80%), Na (1.20%), Mg (0.28%), K (0.31%), Fe (0.32%) and Ca (0.09%).

Struvite precipitation

Struvite precipitation experiments are performed in batch mode using 1 L reactor. Firstly, 500 mL of landfill leachate is poured in a reactor kept over the magnetic stirrer. Then necessary quantity of sewage sludge and Mg source is added to the reactor for struvite formation. Further the whole solution is mixed properly at 300 rpm for 90 min. During the mixing process, 5 mL of supernatant is collected at regular time intervals for further analysis. The precipitates are collected and then washed thrice with deionized water, later oven dried at 35°C for 48 h.

Analytical techniques

The composition of the landfill leachate is measured as per standard methods (APHA 2012). The pH of the solution is computed using pH meter (827 pH lab, Metrohm). The concentration of phosphate in the solution is analyzed using vanadomolybdophosphoric acid spectrometric technique with UV/VIS spectrometer (Lambda 35, PerkinElmer). The Mg²⁺ concentration in the solution is determined using atomic absorption spectrometer (pinaacle 900T, PerkinElmer). The precipitates collected after the experiments are oven dried at 35°C for 48 h. The surface morphology of the dried precipitates is determined using Scanning Electron Microscope (SEM; JEOL, JMT-300). The obtained precipitates is analysed using X-ray Diffractometer (XRD; Rigaku, D-Max/ Ultima III). Dynamic Light Scattering (DLS; LS230, Beckman Coulter) technique is used to measure the particle size of the collected precipitates. Furthermore, the composition of seed material is examined using energy-dispersive X-ray spectrometer (EDS). In addition to that heavy metal content and composition of the obtained precipitate is measured by adding concentrated nitric acid to the deionized water containing obtained precipitate. Then, heavy metal contents are analyzed using ICP-MS. Additionally, the saturation index (SI) of salts is evaluated using the below equation (2).

$$SI = \log \frac{IAP}{K_{sp}} \tag{2}$$

where IAP is the ion activity product and K_{sp} is the saturation product of the salts respectively. SI > 0 implies that the solution is in super saturated condition and spontaneous precipitation occurs within the system. Similarly, SI < 0 implies that under saturated condition exist in the solution and it does not favor the precipitation formation. Likewise, SI = 0 indicates that the solution is in equilibrium state. The purity of the precipitates obtained after the experiments is calculated using equation (3).

$$\text{Purity (\%)} = \frac{M_{\text{Struvite}}}{M_{\text{Total precipitate}}} * 100 \tag{3}$$

where M_{Struvite} and M_{Total precipitate} correspond to struvite mass and total precipitate mass respectively. All the studies are carried out in triplicates and the average value is reported.

Optimization using RSM

In the current study, optimization of the whole process is carried out using RSM with Design Expert 11.0 software. Moreover, Box-Behnken Design (BBD) is employed to investigate the individual and as well combined influence of factors on response. The individual parameters that are considered for the experimental design with codes and ranges are given in Table 2. The experimental data is fitted with second order polynomial equation given below.

$$Y = \alpha_0 + \sum_{i=1}^4 \alpha_i x_i + \sum_{i=1}^4 \alpha_{ii} x_i^2 + \sum_{i=1}^4 \alpha_{ij} x_i x_j \tag{4}$$

where Y is the response value (recovery efficiency (%)), α₀ is the intercept, α_i is the linear coefficient, α_{ii} is the quadratic coefficient, and α_{ij} is the interaction coefficient. In addition to that analysis of variance (ANOVA) is also performed to examine the quality of the model developed. Based on the probability value (p – value) obtained from the ANOVA analysis,

Table 2 Levels and code of individual factors considered for experimental design

Parameter	Code	Levels		
		-1	0	+1
pH	A	8	9.5	11
Seed dose (g/L)	B	5	17.5	30
Ca:Mg molar ratio	C	0.1	1.05	2
Na:Mg molar ratio	D	0.5	1.75	3

factors or individual variables are categorized as significant or insignificant.

Chemical equilibrium modeling

Chemical-equilibrium models are most widely employed to predict the precipitation potential of struvite from aqueous solutions (Scott et al. 1991; Wang et al. 2006b). Visual MINTEQ is commonly used chemical equilibrium modeling tool and also possess database of huge equilibrium constants. Visual MINTEQ is majorly employed to find solubility, equilibrium between solid and dissolved phases and speciation of ions in the solution (Çelen et al. 2007). In addition to that various salts that might precipitate due to interaction between different ions can also be determined using Visual MINTEQ. Additionally, SI of salts also can be computed using this model. The activity coefficients estimation by the model is according to Davies approximation of the Debye–Huckel equation.

Results and discussion

Characteristics of landfill leachate

The landfill leachate used in the present study is rich in NH_4^+ -N content when compared to PO_4^{3-} -P and Mg^{2+} (From Table 1) and also NH_4^+ -N: PO_4^{3-} -P concentration ratio is 39.75. Even though leachate contains greater concentration of NH_4^+ -N, the concentration of Mg^{2+} and PO_4^{3-} -P required to precipitate struvite is low. Hence addition of PO_4^{3-} -P and Mg^{2+} sources is imperative and are supplied using sewage sludge and MgO respectively.

Effect of pH on recovery efficiency

pH is one of the most governing factor that influences the struvite formation and also it effects the speciation of ions (PO_4^{3-} -P, Mg^{2+} , NH_4^+ -N) that are responsible for struvite formation (Zhou and Wu 2012). Moreover, pH also impacts the super saturation and solubility of salts that are likely to form during the precipitation process (Le Corre et al. 2009). In addition to that pH predominantly affects the particle size of the precipitates formed. Therefore, in this study the impact of pH (8–11) on NH_4^+ -N, PO_4^{3-} -P and Mg^{2+} recovery efficiency, struvite purity, size of the precipitate, SI and the amount of precipitate formed is determined and the results are presented in Fig. 1.

From the Fig. 1a, it is observed that the PO_4^{3-} -P and NH_4^+ -N recovery efficiency is notably influenced by pH of the solution. Both PO_4^{3-} -P and NH_4^+ -N recovery efficiencies increased up to pH 9.5 and then maximum is attained at pH 9.5. While for pH beyond 9.5, PO_4^{3-} -P and NH_4^+ -N recovery

efficiency is reduced with increased pH. At pH 9.5, the PO_4^{3-} -P and NH_4^+ -N recovery efficiency achieved is 86.9% and 78.9% respectively. Furthermore, Mg^{2+} recovery efficiency is rising rapidly for a pH range of 8–11. The maximum Mg^{2+} recovery efficiency of 91.5% is obtained at pH 11. The purity of the struvite precipitate is dropped from 88.6% to 66.5% with pH (Fig. 1c).

Struvite formation is mainly impacted by pH of the solution (Huang et al. 2015). pH plays an essential role in controlling the speciation of struvite constituent ions. In general, phosphate species prevail in the form of PO_4^{3-} , HPO_4^{2-} , and H_2PO_4^- depending upon pH of the system (Rathod et al. 2014). H_2PO_4^- species would be present in the solution at pH 5 to 6.5. Likewise, HPO_4^{2-} species would exist at a pH range of 7 to 9 and PO_4^{3-} species would be available in the solution at pH >10. From pH 7 to 9 due to availability of HPO_4^{2-} ions and also lower H^+ concentration facilitated the struvite precipitation; this ultimately leads to greater PO_4^{3-} -P recovery efficiency. Additionally, for pH >10, the conversion of NH_4^+ to NH_3 would not favor the struvite precipitation, thereby results in lower PO_4^{3-} -P and NH_4^+ -N recovery efficiency. On the other hand at pH >10, the Mg^{2+} ions will react with OH^- and PO_4^{3-} ions exist in the solution and forms $\text{Mg}(\text{OH})_2$ and $\text{Mg}_3(\text{PO}_4)_2$ respectively. Hence, Mg^{2+} recovery is enhanced with increased pH.

Additionally, Visual MINTEQ is utilized to correlate the results obtained from the experiments. The results of Visual MINTEQ are shown in Fig. 1b. SI of salts that are likely to form in the solution is computed using Visual MINTEQ 3.1. At pH 8, struvite and $\text{Ca}_4\text{H}(\text{PO}_4)_3 \cdot 3\text{H}_2\text{O}$ are precipitated in the solution this represents that oversaturated condition prevails for both the salts in solution. Until pH 9.5 the SI of struvite increased; maximum SI is achieved at 9.5 and beyond 9.5 SI reduced this indicates that the amount of struvite formed is high at pH 9.5. Therefore, high struvite formation at pH 9.5 is also coincides with the high PO_4^{3-} -P and NH_4^+ -N recovery efficiency (Fig. 1a) attained at pH 9.5. As the pH increases along with struvite other salts like $\text{Mg}_3(\text{PO}_4)_2$, $\text{Mg}(\text{OH})_2$, $\text{MgHPO}_4 \cdot 3\text{H}_2\text{O}$ and $\text{Ca}_4\text{H}(\text{PO}_4)_3 \cdot 3\text{H}_2\text{O}$ are also formed in the solution. But $\text{MgHPO}_4 \cdot 3\text{H}_2\text{O}$ salt is in dissolved state (i.e under saturated) from pH 8 to 11, so it does not have any influence on purity of struvite. At higher pH, lower PO_4^{3-} -P recovery efficiency is due to the formation of $\text{Mg}(\text{OH})_2$ in the solution. Hence, the availability of Mg^{2+} to form struvite would be reduced. Till pH 11, $\text{Mg}(\text{OH})_2$ is in soluble condition; hence, precipitate formation is not possible within the system. $\text{Mg}_3(\text{PO}_4)_2$ and $\text{Ca}_4\text{H}(\text{PO}_4)_3 \cdot 3\text{H}_2\text{O}$ formation with increased pH reduced the struvite purity. At pH 10, the SI of struvite and $\text{Mg}_3(\text{PO}_4)_2$ is same. Even through the SI is same, the solubility product (K_{sp}) of $\text{Mg}_3(\text{PO}_4)_2$ ($K_{\text{sp}} = 10^{-25}$) (Chen et al. 2018) is lower than struvite ($K_{\text{sp}} = 10^{-13.27}$) (Hanhoun et al. 2011). Thus the precipitation

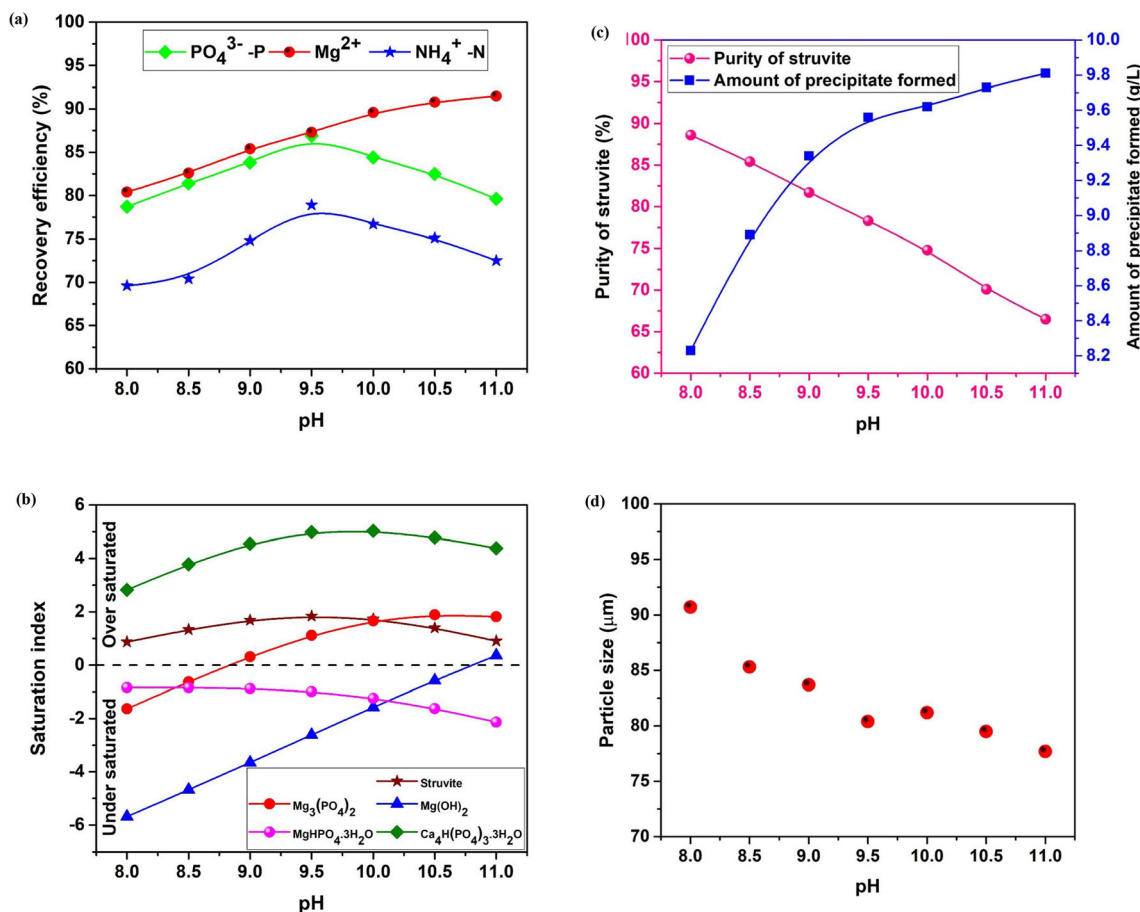


Fig. 1 Variation of (a) PO_4^{3-} -P, NH_4^+ -N and Mg^{2+} recovery efficiency, (b) saturation index (c) purity of struvite and amount of precipitate formed, (d) particle size with pH of the solution

potential of $\text{Mg}_3(\text{PO}_4)_2$ is greater than struvite. Therefore, the purity of struvite is diminished with pH (Fig. 1c). Furthermore, these results are also coinciding with the enhanced amount of precipitate formation with pH (Fig. 1c). From Fig. 1b, it is found that with the pH, the precipitation of salts increased. Thus, the amount of precipitates formed is also enhanced, thereby purity of the struvite is reduced (Fig. 1c).

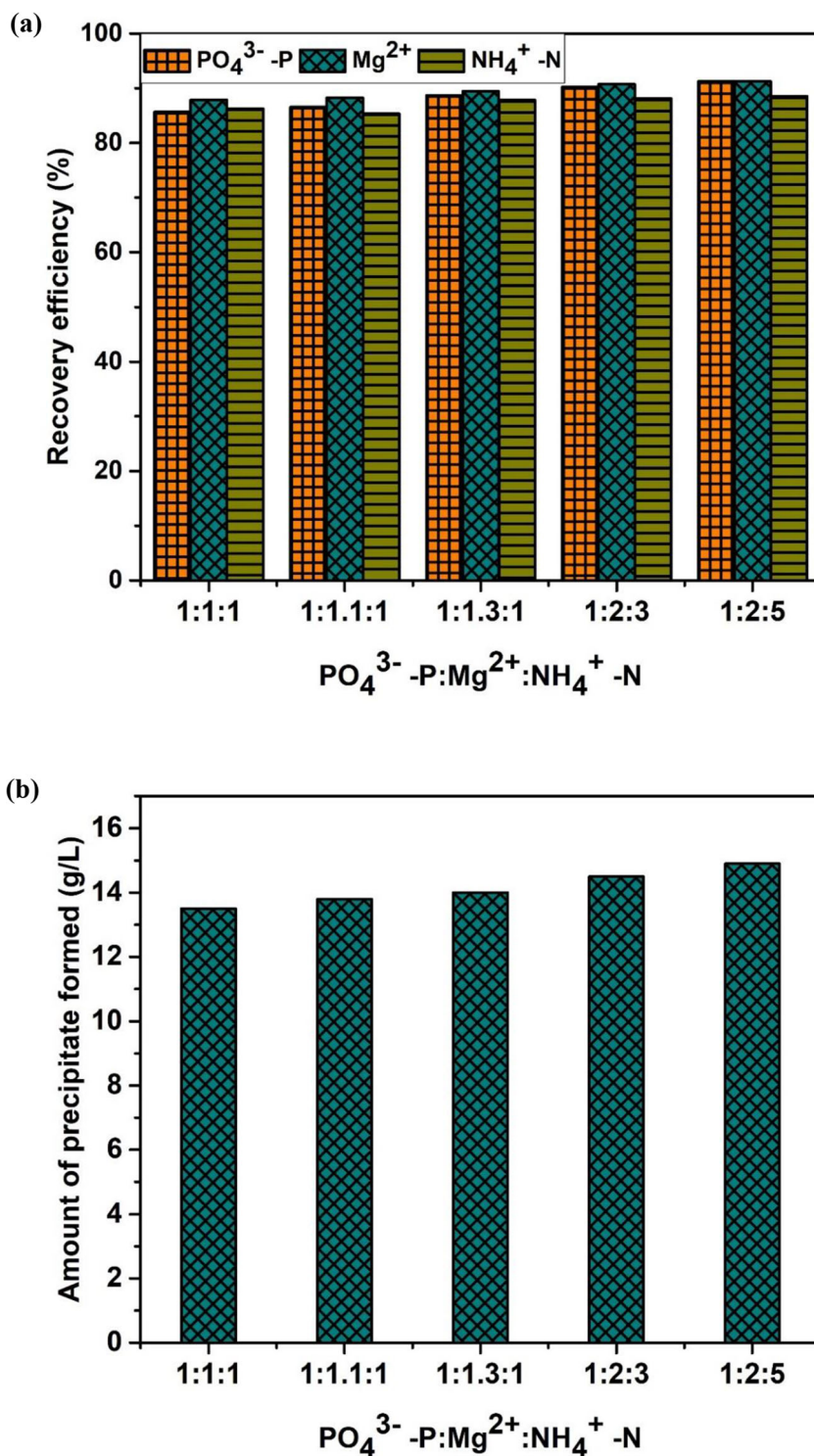
The variation of average particle size of the precipitates obtained after the experiments with pH is shown in Fig. 1d. As pH increased from 8 to 11, the particle size of precipitates is decreased. The reduction in the size is mainly due to super saturation phenomenon of struvite (Fig. 1b). At higher super saturation, nucleation outweighs crystal growth (Ronteltap et al. 2010). Therefore, struvite is formed as small particles rather than larger particles. In addition to that electrostatic repulsion between negatively charged particles also inhibits the agglomeration. As the pH increases, zeta potential becomes further negative and ultimately leads to lower size. These results are similar to the studies conducted by Zhang et al. (2016) and Matynia et al. (2006).

Effect of molar ratio on recovery efficiency

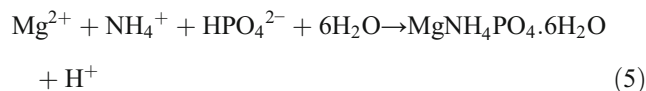
The effect of different molar ratio (PO_4^{3-} -P: Mg^{2+} : NH_4^+ -N) on PO_4^{3-} -P, Mg^{2+} and NH_4^+ -N recovery efficiency at pH 9.5 is depicted in Fig. 2. Furthermore, the quantity of precipitate formed and particle size of the collected precipitates at numerous molar ratios is also determined. The variation of species concentration with pH is also computed (Fig. 3). Additionally, the precipitates formed at various molar ratios and pH 9.5 are characterized using SEM and XRD (Fig. 4).

From Fig. 2a, it is found that at PO_4^{3-} -P: Mg^{2+} : NH_4^+ -N molar ratio of 1:2:5 the recovery efficiency of PO_4^{3-} -P, Mg^{2+} and NH_4^+ -N is 91.2%, 91.2% and 88.5% respectively. This indicates that struvite precipitation take place if the product of constituent ions (PO_4^{3-} -P, Mg^{2+} and NH_4^+ -N) exceeds solubility product (Chen et al. 2018). Moreover, from Fig. 2b also it is observed that the quantity of precipitate is increased with the molar ratio. Even through, the recovery efficiency is high at 1:2:5 molar ratio due to economic consideration 1:1.3:1 is used for further analysis. For the optimized molar ratio of 1:1.3:1, the concentration variation of NH_4^+ , NH_3 ,

Fig. 2 Variation of (a) PO_4^{3-} -P, Mg^{2+} and NH_4^+ -N recovery efficiency, (b) amount of precipitate formed at different PO_4^{3-} -P: Mg^{2+} : NH_4^+ -N molar ratios and at pH 9.5

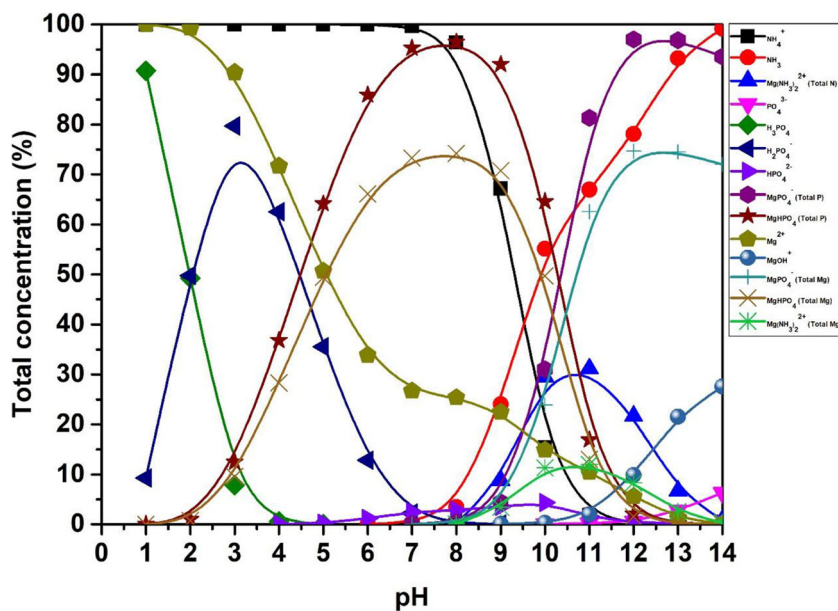


$\text{Mg}(\text{NH}_3)_2^{2+}$ (Total N), PO_4^{3-} , H_3PO_4 , H_2PO_4^- , HPO_4^{2-} , $\text{Mg}(\text{PO}_4)^-$ (Total P), MgHPO_4 (Total P), Mg^{2+} , MgOH^+ , MgPO_4^- (Total Mg), MgHPO_4 (Total Mg), $\text{Mg}(\text{NH}_3)_2^{2+}$ (Total Mg) at different pH is computed (Fig. 3). Figure 3 depicts that HPO_4^{2-} is the dominating species from pH 8 to 11 than H_2PO_4^- and PO_4^{3-} . Therefore, the struvite formation occurs according to below equation.



The particle size (D (90%)) of the precipitates collected at 1:1:1, 1:1.1:1, 1:1.3:1, 1:2:3 and 1:2:5 is 91.4 μm , 90.5 μm , 90.7 μm , 87.4 μm and 89.2 μm respectively. The particle size

Fig. 3 Variation of total concentration of ions at different pH for PO_4^{3-} -P: Mg^{2+} : NH_4^+ -N molar ratio of 1:1.3:1



of precipitates is in the range of 87 μm to 92 μm . Therefore, the molar ratio does not have an impact on the particle size of the precipitates. These results are coinciding with the studies demonstrated by Le Corre et al. (2007) and Warmadewanthi and Liu (2009).

The surface morphology of the collected precipitates at pH 9.5 and different PO_4^{3-} -P: Mg^{2+} : NH_4^+ -N molar ratios is shown in Fig. 4a. The surface of the precipitates is appeared as smooth with needle structure. Similarly, the XRD spectrum of the precipitates is also shown in Fig. 4b. Also, the spectrum

of these precipitates is compared with the standard spectrum (PDF#71-2089) of struvite. XRD spectrum clearly represents that as the molar ratio of PO_4^{3-} -P: Mg^{2+} : NH_4^+ -N increases along with struvite other salts such as $\text{Mg}_3(\text{PO}_4)_2$ and $\text{Ca}_4\text{H}(\text{PO}_4)_3 \cdot 3\text{H}_2\text{O}$ are also formed in the solution.

Effect of seed dose on recovery efficiency

To find the impact of seed dose on recovery efficiency of PO_4^{3-} -P, Mg^{2+} and NH_4^+ -N, seed is added to the solution

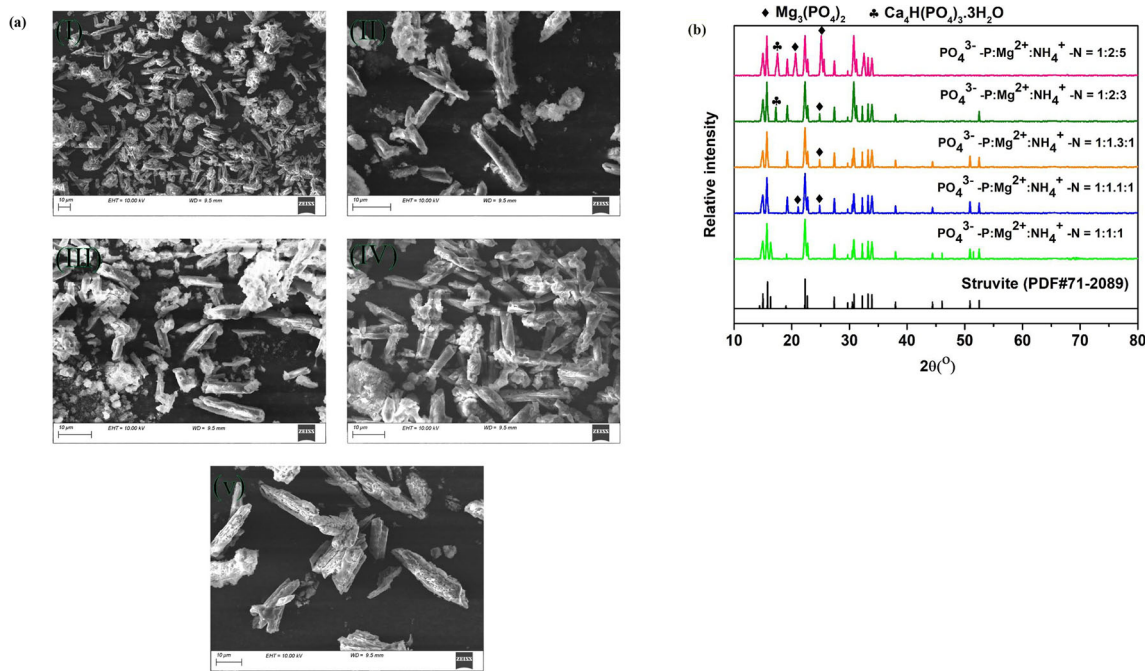


Fig. 4 (a) Surface morphology at molar ratios of (I) 1:1:1 (II) 1:1.1:1 (III) 1:1.3:1 (IV) 1:2:3 and (V) 1:2:5 (b) XRD spectrum of precipitates at different molar ratios and at pH 9.5

at a range from 5 to 30 g/L (Fig. 5). Solution pH of 9.5 and PO_4^{3-} -P: Mg^{2+} : NH_4^+ -N molar ratio of 1:1.3:1 is maintained while conducting the experiments.

The PO_4^{3-} -P, Mg^{2+} and NH_4^+ -N recovery efficiency is increased with an increase in seed dose. However, the variation in recovery efficiency (PO_4^{3-} -P, Mg^{2+} and NH_4^+ -N) at a seed dose of 20 g/L and 30 g/L is insignificant. Therefore, seed dose of 20 g/L is considered as an optimum dose. Struvite precipitate formation occurs in two stages. First stage is nucleation and the second stage is crystal growth (Doyle and Parsons 2002). Former stage is the one in which all the constituent ions (PO_4^{3-} -P, Mg^{2+} and NH_4^+ -N) would attach with each other and form struvite, while the latter stage helps to grow the formed struvite. Nucleation occurs if high supersaturation condition prevails in the solution. Seed material would provide active sites for the constituent ions, hence all ions in the solution will enter immediately into these sites and allows the crystal growth (Liu et al. 2013). Therefore, the availability of active sites is less at lower dose than at higher dose this ultimately helps for achieving high recovery efficiency at higher dose. These results are similar to the studies depicted by Song et al. (2018). The performance of kaolinite is compared with the other seed materials employed for struvite formation is given in Table 3.

Effect of other ions on struvite precipitation

Effect of Ca^{2+}

The impact of Ca^{2+} on PO_4^{3-} -P recovery efficiency, amount of precipitate formation, Ca^{2+} recovery efficiency and SI of different salts is investigated at various Ca:Mg molar ratios

(Fig. 6). While conducting the experiments the pH of the system is maintained at 9.5.

As observed in Fig. 6a, both PO_4^{3-} -P and Ca^{2+} ions recovery efficiency increased as Ca:Mg molar ratio increased. Similarly amount of precipitate formation is also increasing, which represents that Ca^{2+} and PO_4^{3-} -P ions are reacting with each other and forms precipitate. As the Ca:Mg molar ratio increased from 0.1 to 2, the recovery efficiency of PO_4^{3-} -P and Ca^{2+} augmented from 82.8 to 93.1% and 78.7 to 89.7% respectively. Hence, the presence of Ca^{2+} has significant influence on struvite formation.

In addition to that, to validate the above-mentioned results, SI of various salts ($\text{Ca}_3(\text{PO}_4)_2$ (am1), $\text{Ca}_3(\text{PO}_4)_2$ (am2), $\text{Ca}_3(\text{PO}_4)_2$ (beta), $\text{Ca}_4\text{H}(\text{PO}_4)_3 \cdot 3\text{H}_2\text{O}$, CaHPO_4 , $\text{CaHPO}_4 \cdot 2\text{H}_2\text{O}$, hydroxyapatite, $\text{Mg}(\text{OH})_2$, $\text{Mg}_3(\text{PO}_4)_2$, $\text{MgHPO}_4 \cdot 3\text{H}_2\text{O}$ and struvite) is determined using Visual MINTEQ 3.1 (Fig. 6b). The SI of Ca-P ($\text{Ca}_3(\text{PO}_4)_2$, $\text{Ca}_4\text{H}(\text{PO}_4)_3 \cdot 3\text{H}_2\text{O}$, CaHPO_4 , $\text{CaHPO}_4 \cdot 2\text{H}_2\text{O}$, hydroxyapatite) precipitates is increased with Ca:Mg molar ratio, whereas the SI of Mg-P ($\text{Mg}_3(\text{PO}_4)_2$, $\text{MgHPO}_4 \cdot 3\text{H}_2\text{O}$ and struvite) precipitates is reduced. The SI of struvite is reduced with Ca:Mg molar ratio indicates that the Ca^{2+} reacts with PO_4^{3-} -P ions and inhibits the reaction between Mg^{2+} and PO_4^{3-} -P. Furthermore, among all those Ca-P precipitates, hydroxyapatite is the one which is highly interfering in struvite formation. Since, the solubility order of Ca-P is $\text{CaHPO}_4 \cdot 2\text{H}_2\text{O} > \text{CaHPO}_4 > \text{Ca}_4\text{H}(\text{PO}_4)_3 \cdot 3\text{H}_2\text{O} > \text{Ca}_3(\text{PO}_4)_2 > \text{hydroxyapatite}$ (Musvoto et al. 2000). Additionally, formation of these precipitates is also depends on pH of the system. At a pH < 7 only the formation of $\text{CaHPO}_4 \cdot 2\text{H}_2\text{O}$ and CaHPO_4 occurs in the solution (Chäirat et al. 2007). Likewise, $\text{Ca}_4\text{H}(\text{PO}_4)_3 \cdot 3\text{H}_2\text{O}$ would precipitate in the solution (Koutsoukos 2001). Similarly, $\text{Ca}_3(\text{PO}_4)_2$ and hydroxyapatite would exist in the

Fig. 5 Variation of PO_4^{3-} -P, Mg^{2+} and NH_4^+ -N recovery efficiency with seed dose at pH 9.5 and PO_4^{3-} -P: Mg^{2+} : NH_4^+ -N molar ratio of 1:1.3:1

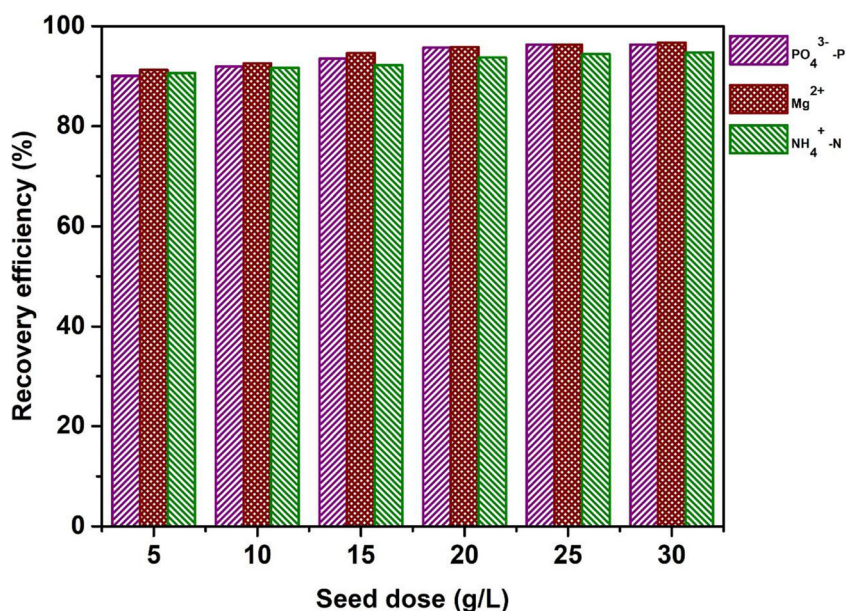
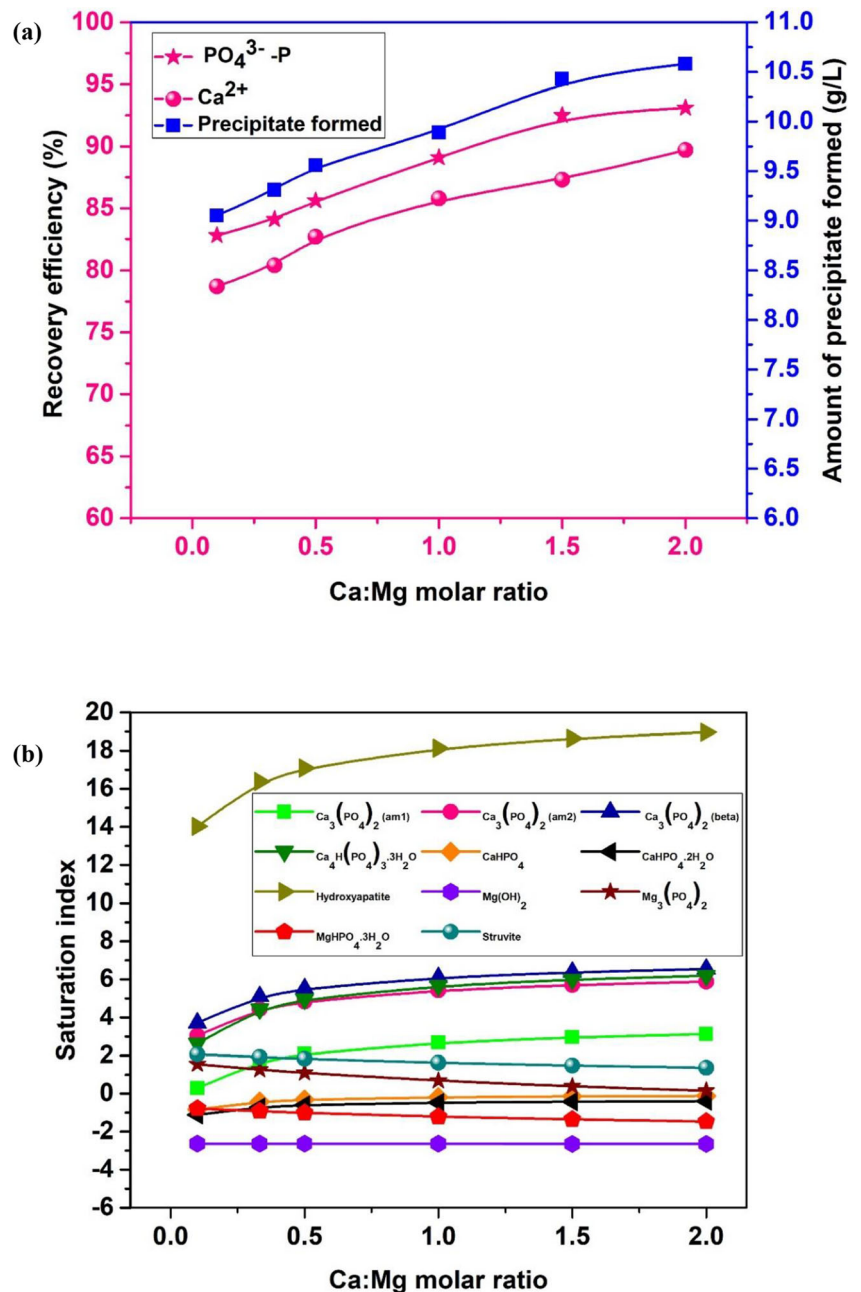


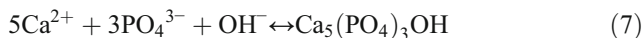
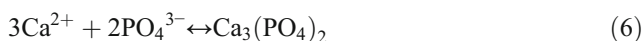
Table 3 Comparison of performance of different seed materials for struvite formation

Seed material	Wastewater used for struvite precipitation	Recovery efficiency obtained (%)		Reference
		NH ₄ ⁺ -N	PO ₄ ³⁻ -P	
Zeolite	Live stock	99	99.9	Min et al. (2019)
Struvite	Synthetic wastewater	91.6	-	Huang et al. (2010)
Struvite	Waste sea water	94	-	Song et al. (2018)
Struvite	Synthetic wastewater	-	89	Wang et al. (2006a)
Struvite	CO ₂ -rich wastewater	-	96	Jordaan et al. (2013)
Kaolinite	Landfill leachate	94.7	96.3	Present study

Fig. 6 Variation of (a) PO₄³⁻ -P, Ca²⁺ recovery efficiency and amount of precipitate formation (b) saturation index of salts at pH 9.5 and with different Ca:Mg molar ratios



solution, when the solution pH is between 9 and 11 (Pastor et al. 2008). Therefore, at an experiment pH of 9.5 $\text{Ca}_3(\text{PO}_4)_2$ and hydroxyapatite are the dominant species and the same is observed in Fig. 6b also. The reactions for $\text{Ca}_3(\text{PO}_4)_2$ and hydroxyapatite formation are given below. Moreover, these two precipitates are responsible for attaining high PO_4^{3-} -P and Ca^{2+} recovery efficiency



Therefore, it is necessary to control the Ca^{2+} in the solution otherwise it will interfere in the struvite formation.

Effect of Na^+

To examine the effect of Na^+ on struvite precipitation, experiments are conducted with various Na:Mg molar ratio (Fig. 7). While conducting the experiments, pH is maintained as 9.5.

Figure 7 illustrates that both PO_4^{3-} -P and Na^+ recovery efficiency enhanced significantly with Na:Mg molar ratio this indicates that amount of Na concentration in the precipitates is enhanced with molar ratio. Consequently, the purity of precipitates might be reduced and also arrest the struvite formation. As Na:Mg molar ratio elevated from 0.5 to 3, the recovery efficiency of Na^+ increased from 58.4 to 65.2%. Occurrence of Na^+ not only reduced the struvite formation but also inhibited $\text{Mg}_3(\text{PO}_4)_2$ precipitation. Furthermore, greater Na^+ concentration promotes the precipitation of $\text{MgNaPO}_4 \cdot 7\text{H}_2\text{O}$ (i.e., Na-struvite) rather than $\text{MgNH}_4\text{PO}_4 \cdot 6\text{H}_2\text{O}$. Therefore, higher Na^+ content in solution promotes Na-struvite reaction, which is beneficial to the Na-struvite precipitation (Gao et al. 2018).

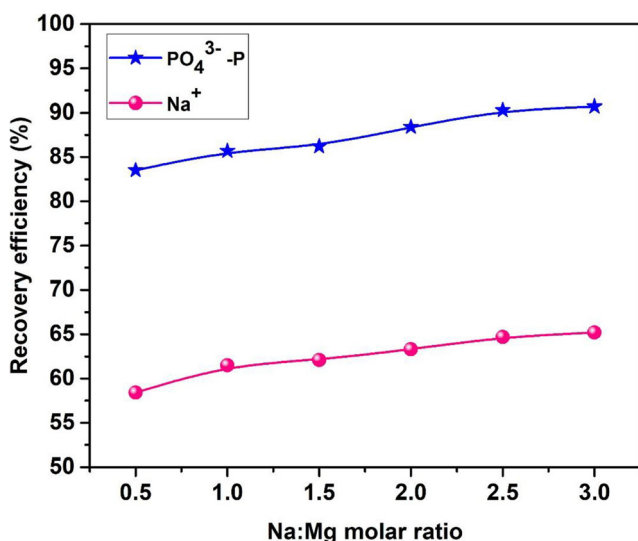


Fig. 7 Variation of PO_4^{3-} -P, Na^+ recovery efficiency with different Na:Mg molar ratios and at pH 9.5

Process optimization using RSM

To optimize the whole process BBD of RSM is utilized. Based on the input data given in Table 2, BBD matrix is developed and the actual and predicted output values are given in Table 4.

The data provided in the BBD matrix is analyzed using Design Expert 11.0. Fit summary results (Table 5) illustrate that quadratic model is best suited with the data than other models. The response value in terms of coded factors is provided in equation (8). The predicted PO_4^{3-} -P recovery efficiency agrees with experimentally calculated PO_4^{3-} -P recovery efficiency for the same set experimental conditions. The results of the ANOVA analysis are given in Table 6.

$$Y = 91.70 - 5.22A + 2.39B + 0.2583C + 0.1500D + 0.0750AB - 0.0250AC + 0.1000AD + 0.0500BC + 0.1000BD + 0.0500CD - 18.32A^2 - 0.0875B^2 - 0.1875C^2 - 0.5000D^2 \quad (8)$$

where $Y = \text{PO}_4^{3-}$ -P recovery efficiency (%), $A = \text{pH}$, $B = \text{seed dose}$, $C = \text{Ca:Mg molar ratio}$, $D = \text{Na:Mg molar ratio}$.

ANOVA results in Table 6 demonstrated that quadratic model developed is significant with F -value of 189.36. Furthermore, the predicted R^2 of 0.9697 is in reasonable agreement with the adjusted R^2 of 0.9895. Adequate precision of 39.0579 (desirable value > 4) represents that adequate signal and the model can be used to navigate the design space. In addition to that the predicted and actual values (Fig. 8) are in best agreement with each other. Therefore, based on the above-mentioned conditions, it is revealed that the developed quadratic model statistically valid.

Interaction influence of independent variables on response

The interaction influence of independent variables on response is evaluated using 3D surface plots as shown in Fig. 9a–f.

Figure 9a illustrates the interaction influence of pH and seed dose on PO_4^{3-} -P recovery efficiency. At a low pH, the influence of seed dose on PO_4^{3-} -P recovery efficiency is negligible. However, pH above 9, the PO_4^{3-} -P recovery efficiency significantly enhanced with the addition of seed dose. Similarly, for pH above 10, the seed does not have an impact on PO_4^{3-} -P recovery efficiency. The major reason for negligible influence of varying seed doses at lower and as well as

Table 4 BBD matrix and the actual and predicted output values

Run	Factor 1 A:pH	Factor 2 B:Seed dose (g/L)	Factor 3 C:Ca:Mg molar ratio	Factor 4 D:Na:Mg molar ratio	Response 1	
					PO ₄ ³⁻ -P recovery efficiency (%)	
					Actual value	Predicted value
1	8	30	1.05	1.75	79.3	80.82
2	11	17.5	1.05	3	68.1	67.91
3	9.5	17.5	0.1	0.5	90.6	90.65
4	9.5	17.5	1.05	1.75	91.7	91.70
5	9.5	30	2	1.75	95.1	94.13
6	9.5	17.5	1.05	1.75	91.7	91.70
7	11	17.5	2	1.75	68.3	68.20
8	9.5	5	0.1	1.75	88.4	88.83
9	8	17.5	1.05	0.5	78.4	78.04
10	9.5	17.5	1.05	1.75	91.7	91.70
11	11	17.5	0.1	1.75	67.7	67.74
12	9.5	5	2	1.75	88.9	89.24
13	9.5	17.5	2	0.5	90.8	91.07
14	9.5	30	0.1	1.75	94.4	93.51
15	11	5	1.05	1.75	66.7	65.60
16	9.5	17.5	2	3	91.1	91.47
17	9.5	30	1.05	3	94.7	93.75
18	9.5	30	1.05	0.5	93.8	93.25
19	8	17.5	0.1	1.75	77.9	78.12
20	11	30	1.05	1.75	68.7	70.54
21	11	17.5	1.05	0.5	67.9	67.41
22	9.5	5	1.05	3	88.1	88.77
23	8	17.5	2	1.75	78.6	78.69
24	9.5	17.5	1.05	1.75	91.7	91.70
25	9.5	17.5	0.1	3	90.7	90.85
26	9.5	5	1.05	0.5	87.6	88.67
27	9.5	17.5	1.05	1.75	91.7	91.70
28	8	5	1.05	1.75	77.6	76.19
29	8	17.5	1.05	3	78.2	78.14

higher pH is due to constrained struvite formation. Therefore, adjusting seed dose at lower and higher pH does not enhance the recovery efficiency. As displayed in Fig. 9b, the effect of different Ca:Mg molar ratio on PO₄³⁻-P recovery efficiency is

insignificant at a lower pH value. At higher pH, increased PO₄³⁻-P recovery efficiency for all Ca:Mg molar ratios is due to the formation of Ca₃(PO₄)₂ and hydroxyapatite. As illustrated in Fig. 9c, at lower and as well as at higher pH,

Table 5 Fit summary results

Source	Sequential <i>p</i> -value	Adjusted R ²	Predicted R ²	
Linear	0.4212	0.0016	-0.2848	
2FI	1.0000	-0.3311	-1.5852	
Quadratic	< 0.0001	0.9895	0.9697	Suggested
Cubic	0.0056	0.9983	0.9477	Aliased

Table 6 ANOVA analysis

Source	Sum of Squares	df	Mean Square	F-value	p-value	
Model	2732.96	14	195.21	189.36	< 0.0001	significant
A-pH	326.56	1	326.56	316.78	< 0.0001	
B- Seed dose (g/L)	68.64	1	68.64	66.58	< 0.0001	
C- Ca:Mg molar ratio	0.8008	1	0.8008	0.7768	0.3930	
D- Na:Mg molar ratio	0.2700	1	0.2700	0.2619	0.6168	
AB	0.0225	1	0.0225	0.0218	0.8847	
AC	0.0025	1	0.0025	0.0024	0.9614	
AD	0.0400	1	0.0400	0.0388	0.8467	
BC	0.0100	1	0.0100	0.0097	0.9229	
BD	0.0400	1	0.0400	0.0388	0.8467	
CD	0.0100	1	0.0100	0.0097	0.9229	
A ²	2178.20	1	2178.20	2112.92	< 0.0001	
B ²	0.0497	1	0.0497	0.0482	0.8294	
C ²	0.2280	1	0.2280	0.2212	0.6454	
D ²	1.62	1	1.62	1.57	0.2303	
Residual	14.43	14	1.03			
Lack of Fit	14.43	10	1.44			
Pure Error	0.0000	4	0.0000			
Cor Total	2747.39	28				

$$R^2 = 0.9947$$

the influence of Na:Mg molar ratio on PO_4^{3-} -P recovery efficiency is negligible. Fig. 9d and e showed the similar trend for seed dose with Ca:Mg molar ratio and Na:Mg molar ratio on PO_4^{3-} -P recovery efficiency respectively. Higher seed dose with greater Ca:Mg and Na:Mg molar ratios could be helpful

for attaining highest PO_4^{3-} -P recovery efficiency. As depicted in Fig. 9f, at higher Na:Mg molar ratio, desired PO_4^{3-} -P recovery efficiency would be obtained over a wide Ca:Mg molar ratio. However, at low Na:Mg molar ratio, the Ca:Mg molar ratio for reaching high PO_4^{3-} -P recovery is narrowed down.

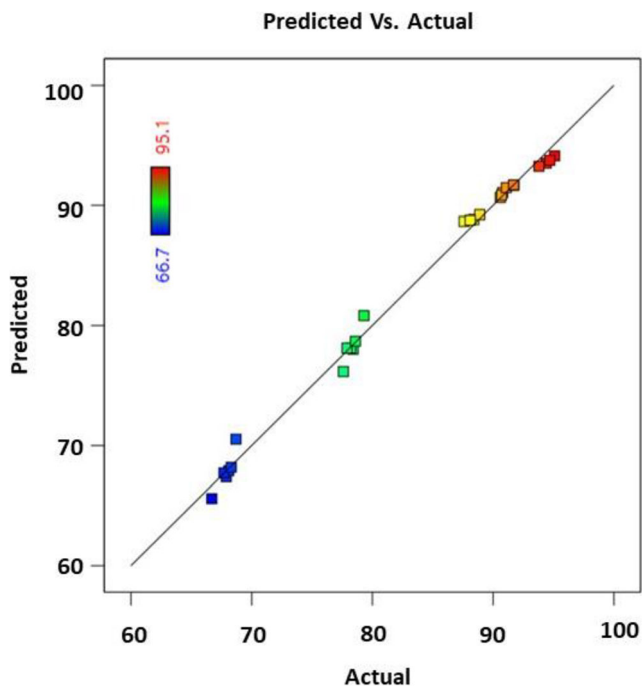


Fig. 8 Correlation of predicted vs actual plot for PO_4^{3-} -P recovery efficiency

Process optimization and validation

In order to assess the best possible conditions of independent parameters, optimization is carried out using desirability function. For maximizing PO_4^{3-} -P recovery efficiency, the independent parameters seed dose, pH, Na:Mg molar ratio and Ca:Mg molar ratio are fixed as targeted criteria in numerical optimization method. Out of all the solutions, the maximum PO_4^{3-} -P recovery efficiency of 94.53% with desirability 0.98 is attained at pH 9.289, seed dose 30 g/L, Na:Mg molar ratio 2.103 and Ca:Mg molar ratio 1.875.

To further validate results obtained through optimization approach, experiments are performed at the above-mentioned conditions and the corresponding PO_4^{3-} -P recovery efficiency is found as 93.12%. Both the predicted and experimental results agree with each other with an error percentage of 1.49 corroborated the RSM results-based optimization and indicated its effectiveness in forecasting the response at other working conditions.

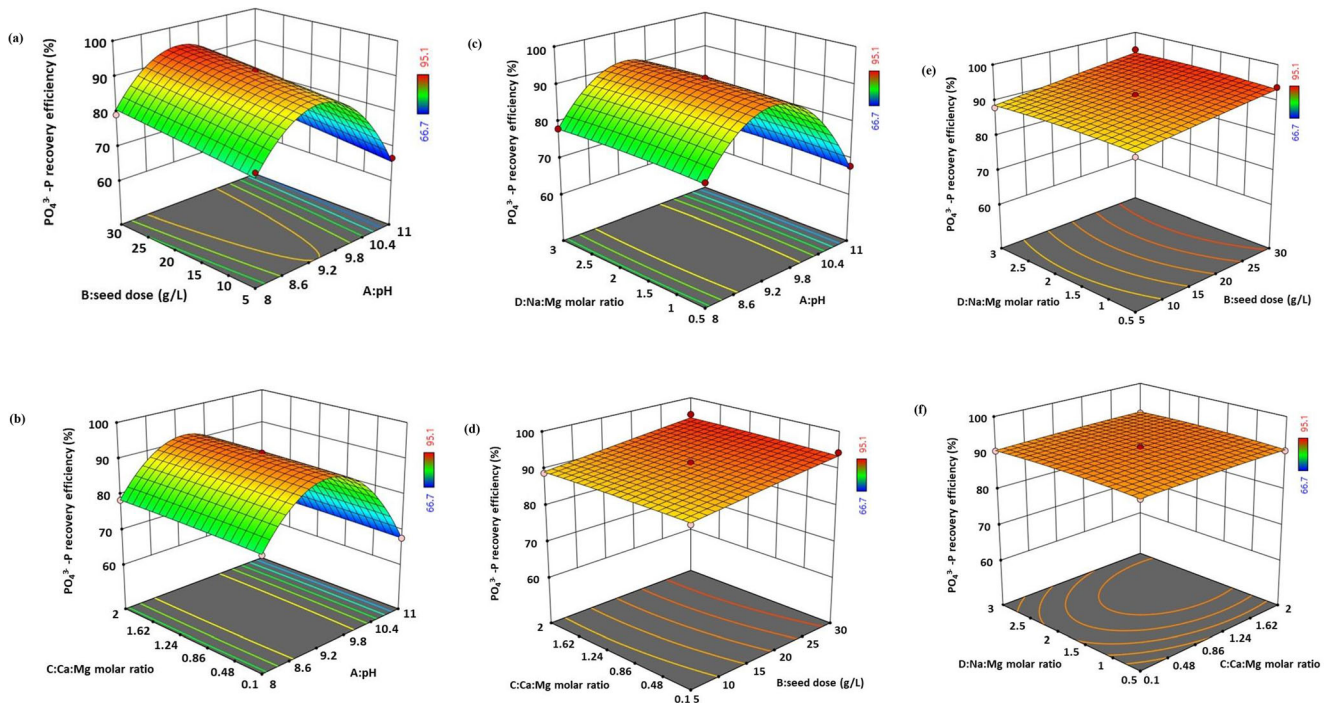


Fig. 9 Interaction influence of (a) pH X seed dose, (b) pH X Ca:Mg molar ratio, (c) pH X Na:Mg molar ratio, (d) seed dose X Ca:Mg molar ratio, (e) seed dose X Na:Mg molar ratio, (f) Ca:Mg molar ratio X Na:Mg molar ratio on PO_4^{3-} -P recovery efficiency

Composition of recovered precipitate and bioavailability

To assess the application of recovered precipitate as a fertilizer, it is substantial to find its composition. Hence, composition of the recovered precipitate at pH 9.5, seed dose 20 g/L and PO_4^{3-} -P:Mg²⁺:NH₄⁺-N molar ratio 1:1.3:1 is determined using ICP-MS (Table 7). The dominant elements are PO_4^{3-} -P (11.4%), Mg²⁺ (9.8%), NH₄⁺-N (4.7%) and Al (4.8%) followed by Na, Ca, and Fe.

Furthermore, the contents of PO_4^{3-} -P, Mg²⁺ and NH₄⁺-N in the obtained precipitates are compared with the theoretical

values (Table 8). The higher Mg content might be due to the formation of other salts like Mg₃(PO₄)₂, and MgHPO₄·3H₂O. Formation Mg-P precipitates mainly depends on pH and concentration of ions and also competitive to struvite formation (Tansel et al. 2018).

The percentage of struvite present in the formed precipitates is computed using NH₄⁺-N concentration in the precipitate, since interaction of NH₄⁺-N is essential for struvite formation (Thant Zin and Kim 2019). In the current study 82.5% of struvite is present in the precipitate. Zhang et al. (2010) reported that 78% of struvite content is available in the precipitates recovered from anaerobically digested dairy effluents.

Bioavailability is one of the essential factors of a fertilizer. The bioavailable PO_4^{3-} -P fraction is generally considered as the soluble PO_4^{3-} -P in 2% citric acid (Wang et al. 2012). The precipitates in the present study possess 89.3% PO_4^{3-} -P bioavailability this represents that PO_4^{3-} -P is easily available to the plants if the obtained precipitate is used as a fertilizer. Commercially available single super phosphate possesses 87% PO_4^{3-} -P bioavailability. Therefore, these results represent that the obtained precipitates contain struvite and are bioavailable in nature.

Table 7 Composition of recovered precipitate

Element	Quantity (g/Kg of sample)
PO_4^{3-} -P	114.3
Mg ²⁺	98.4
NH ₄ ⁺ -N	46.7
Al	48.5
Fe	0.7
Ca	8.4
Na	13.7
Cu	0.0012
Ni	0.0001
Cd	0.00001

* Measured using standard methods (APHA 2012)

Economic feasibility

Struvite production at an industrial level is difficult because of high chemical costs. Therefore, it is necessary to use alternate economically viable resources for struvite production to

Table 8 Comparison of composition and molar ratio of obtained precipitate with theoretical value

	Mass content (%)			Molar ratio
	PO ₄ ³⁻ -P	Mg ²⁺	NH ₄ ⁺ -N	PO ₄ ³⁻ -P:Mg ²⁺ :NH ₄ ⁺ -N
Theoretical value (Struvite)	12.6	9.9	5.7	1:1:1
Obtained precipitate	11.4	9.8	4.7	1:1.1:0.9

minimize the chemical costs. In the current study leachate is used as an NH₄⁺-N source and sewage sludge is used as PO₄³⁻-P source rather than chemicals. However, the usage of Mg²⁺ source is not possible to avoid, but optimizing its dose would be helpful to reduce the cost. Hence, economic feasibility of the present study is computed through economic calculation. During the evaluation, the cost incurred due to chemicals alone is considered while the investment, maintenance and manpower cost is not considered. However, the income generated by selling the struvite is considered in economic evaluation.

The conditions that are considered for the economic estimation are pH 9.5, seed dose 20 g/L and PO₄³⁻-P:Mg²⁺:NH₄⁺-N molar ratio 1:1.3:1. The overall cost incurred due to chemicals is given in Table 9.

The total amount of precipitate formed per m³ of wastewater is 527.5 Kg. The purity of struvite is 82.5%, hence the quantity of struvite precipitate is 435.1 kg/m³. The selling price of struvite is 420\$/ton; hence, the income obtained by selling the struvite is 182.74\$. A total amount of 159.5\$ can be gained as a profit using struvite precipitation method in this study. In addition to that struvite precipitation technique further minimized the sludge disposal cost.

Conclusion

NH₄⁺-N present in landfill leachate recovery as struvite by adding waste resource sewage sludge as PO₄³⁻-P source and MgO as Mg²⁺ source is greatly feasible. Solution pH is a dominating parameter influenced struvite precipitation and the optimum pH is obtained as 9.5. Purity of struvite formed and the particle size is reduced as the pH increased from 8 to 11. Similarly, the amount of precipitate formed increased with pH. The PO₄³⁻-P:Mg²⁺:NH₄⁺-N molar ratio of 1:1.3:1 is considered as optimum ratio for struvite formation.

Table 9 Overall chemical cost

Chemical name	Market price (\$/Kg)	Overall price (\$/m ³)
Kaolinite	0.13	2.64
MgO	0.40	20.54
Total cost		23.18

Additionally, the recovery efficiency of PO₄³⁻-P, Mg²⁺ and NH₄⁺-N enhanced significantly with seed addition at pH 9.5. Presence of Ca²⁺ and Na⁺ ions in the solution inhibited the struvite formation. RSM based optimization would be helpful for forecasting PO₄³⁻-P recovery efficiency at other operating conditions. The high struvite content (82.5%) and PO₄³⁻-P bioavailability (89.3%) suggested that the formed precipitate can be used as a fertilizer. Economic evaluation also illustrated that the struvite precipitation is economically feasible with a profit of 159.5\$/m³.

Author contribution AL formulated the methodology, performed the experiments and analysis, and interpreted the data obtained from the analysis. In addition to that writing the original draft, critical review, editing and revision of the manuscript was accomplished by AL. SKTR provided the resources required to conduct the experiments, validated the results and supervised the present study. All authors have read and approved the final manuscript.

Data availability The datasets used and/or analyzed during the current study are available from the corresponding author on reasonable request.

Declarations

Ethics approval and consent to participate Not applicable

Consent for publication Not applicable

Competing interests The authors declare no competing interests.

References

- Ahmed FN, Lan CQ (2012) Treatment of landfill leachate using membrane bioreactors: A review. *Desalination* 287:41–54. <https://doi.org/10.1016/j.desal.2011.12.012>
- APHA (2012) Standard methods for the examination of water and wastewater. Washington, DC ISBN 9780875532356
- Çelen I, Buchanan JR, Burns RT, Bruce Robinson R, Raj Raman D (2007) Using a chemical equilibrium model to predict amendments required to precipitate phosphorus as struvite in liquid swine manure. *Water Res* 41:1689–1696. <https://doi.org/10.1016/j.watres.2007.01.018>
- Chairat C, Oelkers EH, Schott J, Lartigue JE (2007) Fluorapatite surface composition in aqueous solution deduced from potentiometric, electrokinetic, and solubility measurements, and spectroscopic observations. *Geochim Cosmochim Acta* 71:5888–5900. <https://doi.org/10.1016/j.gca.2007.09.026>

- Chemlal R, Azzouz L, Kernani R, Abdi N, Lounici H, Grib H, Mameri N, Drouiche N (2014) Combination of advanced oxidation and biological processes for the landfill leachate treatment. *Ecol Eng* 73:281–289. <https://doi.org/10.1016/j.ecoleng.2014.09.043>
- Chen Y, Liu C, Guo L, Nie J, Li C (2018) Removal and recovery of phosphate anion as struvite from wastewater. *Clean Techn Environ Policy* 20:2375–2380. <https://doi.org/10.1007/s10098-018-1607-2>
- Chu H, Hosen Y, Yagi K (2007) NO, N₂O, CH₄ and CO₂ fluxes in winter barley field of Japanese Andisol as affected by N fertilizer management. *Soil Biol Biochem* 39:330–339. <https://doi.org/10.1016/j.soilbio.2006.08.003>
- Corona F, Hidalgo D, Martín-Marroquín JM, Antolín G (2020a) Study of the influence of the reaction parameters on nutrients recovering from digestate by struvite crystallisation. *Environ Sci Pollut Res* 28:24362–24374. <https://doi.org/10.1007/s11356-020-08400-4>
- Corona F, Hidalgo D, Martín-Marroquín JM, Meers E (2020b) Study of pig manure digestate pre-treatment for subsequent valorisation by struvite. *Environ Sci Pollut Res* 28:24731–24743. <https://doi.org/10.1007/s11356-020-10918-6>
- Di Iaconi C, Pagano M, Ramadori R, Lopez A (2010) Nitrogen recovery from a stabilized municipal landfill leachate. *Bioresour Technol* 101:1732–1736. <https://doi.org/10.1016/j.biortech.2009.10.013>
- Doyle JD, Parsons SA (2002) Struvite formation, control and recovery. *Water Res* 36:3925–3940. [https://doi.org/10.1016/S0043-1354\(02\)00126-4](https://doi.org/10.1016/S0043-1354(02)00126-4)
- Gao Y, Liang B, Chen H, Yin P (2018) An experimental study on the recovery of potassium (K) and phosphorus (P) from synthetic urine by crystallization of magnesium potassium phosphate. *Chem Eng J* 337:19–29. <https://doi.org/10.1016/j.cej.2017.12.077>
- Hanhoun M, Montastruc L, Azzaro-Pantel C, Biscans B, Frèche M, Pibouleau L (2011) Temperature impact assessment on struvite solubility product: A thermodynamic modeling approach. *Chem Eng J* 167:50–58. <https://doi.org/10.1016/j.cej.2010.12.001s>
- Huang H, Xiao X, Yang L, Yan B (2010) Recovery of nitrogen from saponification wastewater by struvite precipitation. *Water Sci Technol* 61:2741–2748. <https://doi.org/10.2166/wst.2010.060>
- Huang H, Liu J, Ding L (2015) Recovery of phosphate and ammonia nitrogen from the anaerobic digestion supernatant of activated sludge by chemical precipitation. *J Clean Prod* 102:437–446. <https://doi.org/10.1016/j.jclepro.2015.04.117>
- Huang H, Liu J, Xu C, Gao F (2016) Recycling struvite pyrolysate obtained at negative pressure for ammonia nitrogen removal from landfill leachate. *Chem Eng J* 284:1204–1211. <https://doi.org/10.1016/j.cej.2015.09.080>
- Jordaen EM, Rezanja B, Çiçek N (2013) Investigation of chemical-free nutrient removal and recovery from CO₂-rich wastewater. *Water Sci Technol* 67:2195–2201. <https://doi.org/10.2166/wst.2013.116>
- Kochany J, Lipczynska-Kochany E (2009) Utilization of landfill leachate parameters for pretreatment by Fenton reaction and struvite precipitation-A comparative study. *J Hazard Mater* 166:248–254. <https://doi.org/10.1016/j.jhazmat.2008.11.017>
- Koutsoukos PG (2001) Current knowledge of calcium phosphate chemistry and in particular solid surface-water interface interactions. In: *Proceedings of the Second International Conference on Phosphorus Recovery for Recycling from Sewage and Animal Wastes*, 12-14 March. Noordwijkerhout, Holland, pp 1–11
- Lavanya A, Sri Krishnaperumal Thanga R (2020) Effective removal of phosphorus from dairy wastewater by struvite precipitation: process optimization using response surface methodology and chemical equilibrium modeling. *Sep Sci Technol* 56:395–410. <https://doi.org/10.1080/01496395.2019.1709080>
- Lavanya A, Ramesh ST, Nandhini S (2019) Phosphate recovery from swine wastewater by struvite precipitation and process optimization using response surface methodology. *Desalin Water Treat* 164:134–143. <https://doi.org/10.5004/dwt.2019.24447>
- Law KP, Pagilla KR (2018) Phosphorus Recovery by Methods Beyond Struvite Precipitation. *Water Environ Res* 90:840–850. <https://doi.org/10.2175/106143017X15131012188006>
- Le Corre KS, Valsami-Jones E, Hobbs P, Jefferson B, Parsons SA (2007) Agglomeration of struvite crystals. *Water Res* 41:419–425. <https://doi.org/10.1016/j.watres.2006.10.025>
- Le Corre KS, Valsami-Jones E, Hobbs P, Parsons SA (2009) Phosphorus recovery from wastewater by struvite crystallization: A review. *Crit Rev Environ Sci Technol* 39:433–477. <https://doi.org/10.1080/10643380701640573>
- Liu Y, Kumar S, Kwag J-H, Ra C (2013) Magnesium ammonium phosphate formation, recovery and its application as valuable resources: a review. *J Chem Technol Biotechnol* 88:181–189. <https://doi.org/10.1002/jctb.3936>
- Matynia A, Koralewska J, Wierzbowska B, Piotrowski K (2006) The influence of process parameters on struvite continuous crystallization kinetics. *Chem Eng Commun* 193:160–176. <https://doi.org/10.1080/009864490949008>
- Min KJ, Kim D, Lee J, Lee K, Park KY (2019) Characteristics of vegetable crop cultivation and nutrient releasing with struvite as a slow-release fertilizer. *Environ Sci Pollut Res* 26:34332–34344. <https://doi.org/10.1007/s11356-019-05522-2>
- Musvoto EV, Wentzel MC, Ekama GA (2000) Integrated chemical-physical processes modelling-II. simulating aeration treatment of anaerobic digester supernatants. *Water Res* 34:1868–1880. [https://doi.org/10.1016/S0043-1354\(99\)00335-8](https://doi.org/10.1016/S0043-1354(99)00335-8)
- Pastor L, Mangin D, Barat R, Seco A (2008) A pilot-scale study of struvite precipitation in a stirred tank reactor: Conditions influencing the process. *Bioresour Technol* 99:6285–6291. <https://doi.org/10.1016/j.biortech.2007.12.003>
- Rani A, Negi S, Hussain A, Kumar S (2020) Treatment of urban municipal landfill leachate utilizing garbage enzyme. *Bioresour Technol* 297:122437. <https://doi.org/10.1016/j.biortech.2019.122437>
- Rathod M, Mody K, Basha S (2014) Efficient removal of phosphate from aqueous solutions by red seaweed, *Kappaphycus alvarezii*. *J Clean Prod* 84:484–493. <https://doi.org/10.1016/j.jclepro.2014.03.064>
- Renou S, Givaudan JG, Poulain S, Dirassouyan F, Moulin P (2008) Landfill leachate treatment: Review and opportunity. *J Hazard Mater* 150:468–493. <https://doi.org/10.1016/j.jhazmat.2007.09.077>
- Ronteltap M, Maurer M, Hausherr R, Gujer W (2010) Struvite precipitation from urine - Influencing factors on particle size. *Water Res* 44:2038–2046. <https://doi.org/10.1016/j.watres.2009.12.015>
- Scott WD, Wrigley TJ, Webb KM (1991) A computer model of struvite solution chemistry. *Talanta* 38:889–895. [https://doi.org/10.1016/0039-9140\(91\)80268-5](https://doi.org/10.1016/0039-9140(91)80268-5)
- Song W, Li Z, Liu F, Ding Y, Qi P, You H, Jin C (2018) Effective removal of ammonia nitrogen from waste seawater using crystal seed enhanced struvite precipitation technology with response surface methodology for process optimization. *Environ Sci Pollut Res* 25:628–638. <https://doi.org/10.1007/s11356-017-0441-0>
- Sun H, Peng Y, Shi X (2015) Advanced treatment of landfill leachate using anaerobic-aerobic process: Organic removal by simultaneous denitrification and methanogenesis and nitrogen removal via nitrite. *Bioresour Technol* 177:337–345. <https://doi.org/10.1016/j.biortech.2014.10.152>
- Tansel B, Lunn G, Monje O (2018) Struvite formation and decomposition characteristics for ammonia and phosphorus recovery: A review of magnesium-ammonia-phosphate interactions. *Chemosphere* 194:504–514. <https://doi.org/10.1016/j.chemosphere.2017.12.004>
- Thant Zin MM, Kim DJ (2019) Struvite production from food processing wastewater and incinerated sewage sludge ash as an alternative N and P source: Optimization of multiple resources recovery by response surface methodology. *Process Saf Environ Prot* 126:242–249. <https://doi.org/10.1016/j.psep.2019.04.018>

- USEPA (2006) Emerging Technologies for Biosolids Management. EPA 832-R-06-005. In: Office of Wastewater Management. U.S. EPA, Washington D.C., U.S.A.
- Wang J, Burken JG, Zhang XJ (2006a) Effect of Seeding Materials and Mixing Strength on Struvite Precipitation. *Water Environ Res* 78: 125–132. <https://doi.org/10.2175/106143005X89580>
- Wang J, Song Y, Yuan P, Peng J, Fan M (2006b) Modeling the crystallization of magnesium ammonium phosphate for phosphorus recovery. *Chemosphere* 65:1182–1187. <https://doi.org/10.1016/j.chemosphere.2006.03.062>
- Wang T, Camps-Arbestain M, Hedley M, Bishop P (2012) Predicting phosphorus bioavailability from high-ash biochars. *Plant Soil* 357: 173–187. <https://doi.org/10.1007/s11104-012-1131-9>
- Warmadewanthi, Liu JC (2009) Selective precipitation of phosphate from semiconductor wastewater. *J Environ Eng* 135:1063–1070. [https://doi.org/10.1061/\(ASCE\)EE.1943-7870.0000054](https://doi.org/10.1061/(ASCE)EE.1943-7870.0000054)
- Yu R, Geng J, Ren H, Wang Y, Xu K (2012) Combination of struvite pyrolysate recycling with mixed-base technology for removing ammonium from fertilizer wastewater. *Bioresour Technol* 124:292–298. <https://doi.org/10.1016/j.biortech.2012.08.015>
- Yu R, Ren H, Wu J, Zhang X (2017) A novel treatment processes of struvite with pretreated magnesite as a source of low-cost magnesium. *Environ Sci Pollut Res* 24:22204–22213. <https://doi.org/10.1007/s11356-017-9708-8>
- Zhang T, Bowers KE, Harrison JH, Chen S (2010) Releasing Phosphorus from Calcium for Struvite Fertilizer Production from Anaerobically Digested Dairy Effluent. *Water Environ Res* 82:34–42. <https://doi.org/10.2175/106143009X425924>
- Zhang X, Hu J, Spanjers H, van Lier JB (2016) Struvite crystallization under a marine/brackish aquaculture condition. *Bioresour Technol* 218:1151–1156. <https://doi.org/10.1016/j.biortech.2016.07.088>
- Zhou S, Wu Y (2012) Improving the prediction of ammonium nitrogen removal through struvite precipitation. *Environ Sci Pollut Res* 19: 347–360. <https://doi.org/10.1007/s11356-011-0520-6>

Publisher's note Springer Nature remains neutral with regard to jurisdictional claims in published maps and institutional affiliations.